Influence of Maximum Aggregate Size on Dynamic Size Effect of Concrete Under Low Strain Rates: Meso-scale Simulations

JIN Liu, *YANG Wangxian*, *YU Wenxuan*, *DU Xiuli**

Key Laboratory of Urban Security and Disaster Engineering of Ministry of Education, Beijing University of Technology, Beijing 100124, P.R. China

(Received 6 November 2019; revised 8 February 2020; accepted 10 February 2020)

Abstract: This study is to explore the influence of maximum aggregate size (MAS) on the failure and corresponding size effect of concrete materials under low strain rates. The failure process of concrete was simulated by the meso-scale numerical method considering the internal heterogeneity of concrete and strain rate effect. Based on the meso-scale method, the failure behavior of concrete specimens with different structural sizes and MAS was investigated. Also, the influence of MAS on the failure modes, nominal strength and corresponding size effect of concrete were studied at the meso-scale. The simulation results indicated that MAS has an obvious influence on the failure modes of concrete subjected to axial compressive and tensile loads. The nominal tensile strength increased as the MAS increased, while the nominal compressive strength increased first and then decreased as the MAS increases under quasi-static load. In addition, it was found that the size effect on nominal strength of concrete would be weakened with the increase of strain rate. When the applied strain rate reached 1 s^{-1}, the size effect on nominal strength of concrete disappeard. Moreover, the MAS has an ignorable influence on the dynamic size effect of concrete under uniaxial compression and tension.

Keywords: concrete; maximum aggregate size; size effect; dynamic compression; dynamic tension; strain rate

CLC number: TU528.1 **Document code:** A **Article ID:** 1005-1120(2020)01-0027-13

0 Introduction

The mechanical characteristics of concrete change with the structural size, which is so-called size effect. Concrete material belongs to the category of quasi-brittle materials[1], and the non-linearity of its mechanical characteristics is derived from the heterogeneity of internal components[2-3]. The size effect of concrete is mainly affected by its internal components (involving the maximum aggregate size (MAS), initial defect, aggregate distribution, aggregate shape and aggregate strength, etc.)[3]. At present, several size effect laws (SELs) for concrete materials have been established based on the available experimental studies, theoretical analysis and numerical simulations, including Bažant's SEL[1], Weibull's statistical SEL[4] and Carpinteri's multifractal SEL[5], etc. Generally speaking, great efforts have been investigated on the size effect of concrete materials subjected to static loads.

As known, the nominal strength of concrete material depends on many factors, such as cement strength, water-cement ratio, curing conditions, aggregate content, size, etc[6]. Approximately three-quarters of the concrete volume is occupied by aggregate particles. Therefore, aggregate particles have a significant impact on the mechanical performance of concrete material[7]. Many researchers have studied the influence of maximum aggregate size (MAS) on the mechanical behavior of concrete[7,8-12]. Despite the rapid development of concrete and its application in many parts of the world, it still takes a lot of efforts to link the mechanical

*Corresponding author, E-mail address: duxiuli2015@163.com.

How to cite this article: JIN Liu, YANG Wangxian, YU Wenxuan, et al. Influence of maximum aggregate size on dynamic size effect of concrete under low strain rates: Meso-scale simulations[J]. Transactions of Nanjing University of Aeronautics and Astronautics, 2020, 37(1):27-39.

http://dx.doi.org/10.16356/j.1005-1120.2020.01.003

characteristics of aggregates to that of concrete[13]. At present, the understanding of influential mechanism of aggregate particle size is not enough. Previous studies mainly focused on the static mechanical characteristics of concrete while the efforts on the influence of MAS on mechanical characteristics of concrete material under dynamic loads are far from enough.

A large amount of experimental efforts shows that concrete material has a significant strain rate effect under dynamic loads, that is to say, the dynamic failure behavior for concrete material is obviously distinct from static failure behavior, especially for concrete material under high strain rates. The dynamic strength of concrete gets a clear enhancement compared to the static nominal strength under uniaxial tensile and compressive loads[14-15].

As mentioned previously, the nominal strength increases significantly with the increasing strain rate. As for the concrete specimens having different structural sizes, the static strength often decreases with the addition of structural size which is the so-called static size effect. It is of great importance to investigate failure behavior of concrete material with different structural sizes under dynamic loads. Unfortunately, studies on mechanical characteristics of concrete having different structural sizes under dynamic loads is almost blank, and there is even no size effect theory under dynamic loads. Only limited studies have been conducted preliminarily on the dynamic size effect of concrete material: Krauthammer et al.[16] conducted dynamic compressive tests on concrete specimens of different sizes and found that the nominal strength decreases with the structural size increases under dynamic loads, and the size effect under dynamic loads is more significant. By contrast, Wang et al.[17] performed the SHPB axial compressive tests of roller compacted concrete (RCC) and it could be observed that the strength increases with the structural size increasing under dynamic compressive loads. Elfahal and Krauthammer[18] also investigated the size effect on strength of concrete under static and dynamic compression and they found that the loading rate has an obvious influence on the size effect of concrete under compressive loads.

In general, in spite of the above test efforts provide a preliminary understanding on the dynamic SE of concrete, it is far from enough. In addition, it is hard to conduct physical tests to research the dynamic size effect of concrete because of the limitations of test conditions and equipment (especially for the concrete specimens with large structural size under high strain rates). Recently, Jin et al.[19-20] have set up a meso-scale numerical method to research the dynamic size effect of concrete under compressive and tensile loads, and the valuable results show that the dynamic SE is really different from the static size effect of concrete material.

The scope of this study is to research the influence of MAS on dynamic failure behavior and corresponding dynamic size effect of concrete. The failure behavior of concrete specimens (geometrically similar) having different structural sizes (b =100—450 mm) and different MAS ($D_{\max}^{\text{agg}}$=10—30 mm) under different low strain rates ($\dot{\varepsilon}$=10^{-5} s^{-1}—1 s^{-1}) has been modelled by the meso-scale numerical simulation method. Moreover, the numerical results were compared to the SEL proposed by Bažant.

1 Meso-scale Numerical Method

In recent years, compared to macro-scale model, meso-scale modelling approaches, thanks to their ability of describing the heterogeneity of concrete internal components, have been widely utilized to investigate concrete failure process and mechanical behavior[21-23]. Here in this section, the details of meso-scale simulations are presented.

1.1 Computational model

As mentioned in literatures[19-21], concrete material at the meso-scale level could be regarded as a composite material composed of mortar matrix, coarse aggregates and the interface transition zones (ITZs). In this study, the models of square and double-edge notched concrete specimens were built to obtain the axial compressive and tensile failure behavior (Fig. 1). Similar with the studies[24-25], the random aggregate model was applied. Herein, refer-

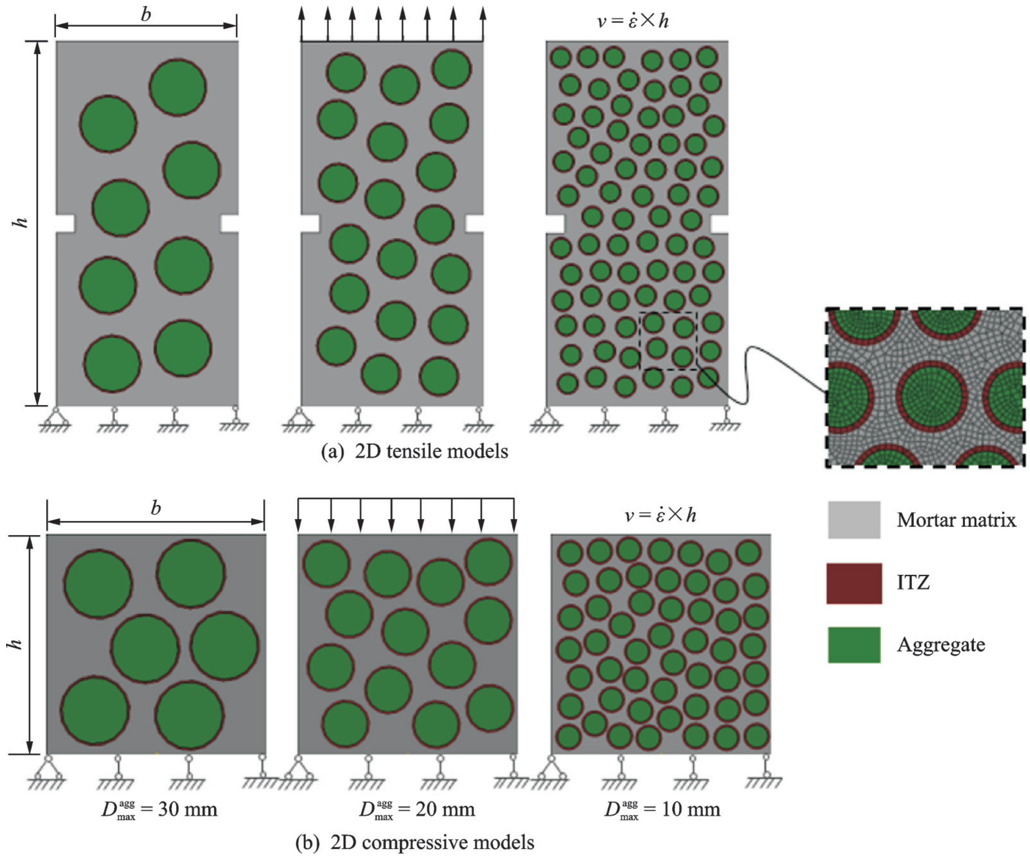

Fig.1 Meso-scale numerical models of concrete

ring to the studies of Sadouki and Wittmann[26] and Cusatis et al.[27], aggregate particles were assumed as circular aggregates. In addition, one-graded concrete was adopted and the maximum aggregate size D_{max}^{agg} is from 10 mm to 30 mm in different models. Furthermore, the volume fraction of aggregate particles was around 40% and the aggregate distribution depended on the Fuller's grading curve for all concrete specimens. The "Take-and-Place" method based on the Monte-Carlo theory[28] was applied to place aggregates in the models randomly. The ITZ phase was regarded as a thin layer around the aggregate particles. Similar to the literatures[21-22,29], the thickness of ITZ was set as 1 mm considering the calculation limitation. The element type was the 4-node quadrilateral element and the average mesh size was set as 1 mm.

The boundary condition and loading condition of numerical model were detailed as follows: the velocity v was employed vertically at the top of numerical model and the strain rate $\dot{\varepsilon}$ mentioned in this study is calculated as the ratio of vertical velocity to specimen height (i. e. $\dot{\varepsilon}=v/h$). Vertical constraint was adopted at the bottom of numerical model, and free boundary was set at other sides of models.

1. 2 Constitutive model

Generally speaking, the ITZs and mortar matrix have similar mechanical characteristics compared to concrete[30]. The plastic damage constitutive model proposed by Lee and Fenves[31] and incorporated in the software of ABAQUS, which could reflect the failure process of the ITZs and mortar matrix, was adopted in the present simulations. This is similar with the previous studies of Jin et al.[29] and Du et al.[25]. Due to cracks may penetrate into the aggregate particles under dynamic loads, similar to the treatment on the ITZ, the mechanical properties of the aggregates could be treated as a kind of mortar matrix with stronger mechanical parameters and thus its dynamic mechanical behavior can also be assumed as similar to those of mortar. Therefore, the plastic damage constitutive model shown in Fig.2 was applied to depict the failure behavior of three-phase components of concrete material.

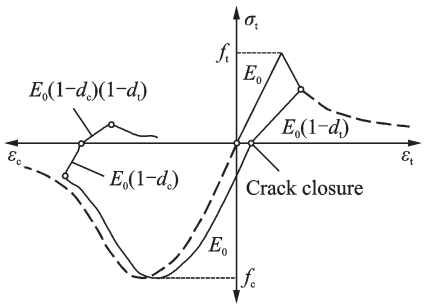

Fig.2 Plastic-damage constitutive model

Compared with concrete strength, other material parameters (e.g. fracture energy, Poisson ratio, elastic modulus, etc.) of concrete are less sensitive to strain rate[32-33]. In view of this, only the amplification effect of material strength was considered. The strain rate effect of concrete components could be represented by the dynamic increasing factor (DIF), which are the same as that in the efforts[21,27,34]. The DIF of the compressive strength (i.e. the CDIF) of concrete recommended by the Comite Euro-international du Beton (CEB)[35] was applied. Moreover, the CEB also gives empirical formula to estimate the dynamic increasing factor in tensile strength (i.e. the TDIF). However, compared with existing test data, the CEB substantially underestimates the TDIF of concrete. Herein, the empirical formula developed by Malvar and Ross[36] was adopted. The detailed introduction of strain rate effect could refer to previous reports[19-20].

1.3 Validation of meso-scale numerical method

Similar with the verified method of Bažant et al.[37], herein the accuracy of numerical calculation was verified by comparing numerical results with test data conducted by Chen et al.[38]. The comparison between the simulated stress-strain curves and Chen et al.'s test results[38] are presented in Fig.3. Moreover, it should be noted that the inversion method (repeated trial algorithm) was employed to determine the material parameters. This means that many mechanical parameters of concrete components should be tried to simulate the failure behavior of concrete and then the most appropriate ones could be selected for further simulations. This treatment is same to that in the literature[29]. When the material parameters listed in Table 1 were applied, the stress-strain curves obtained by numerical simulation were well consistent with the experimental ones[38]. This preliminarily verifies the feasibility of the meso-scale numerical method and the rationality of parameters selection.

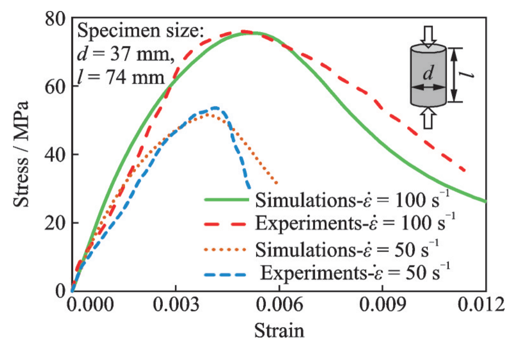

Fig.3 Comparison of the numerical results and Chen's experimental results[38]

Table 1 Material parameters of the concrete

Parameter	Aggregate	ITZ	Mortar matrix
Compressive yield stress σ_c /MPa	80.0^	16.0^	25.0^
Tensile yield stress σ_t /MPa	6^	1.6^	2.5^
Poisson ratio υ	0.16*	0.2*	0.2*
Elastic modulus E /GPa	73*	26*	38*
Dilation angle ψ /(°)	18*	15*	18*
Mass density ρ/(kg•m^{-3})	2 880*	2 750*	2 750*

Parameters with "*" are based on Jin et al.'s reports[19,20]; parameters with "^" are obtained by repeated trial.

Fig.4 presents the failure modes obtained from simulated results and test results of Yan and Lin[39]. It can be seen that the simulated failure modes are closely similar to the experimental ones. This demonstrates that the present meso-scale numerical method can well analyze the failure behavior of con-

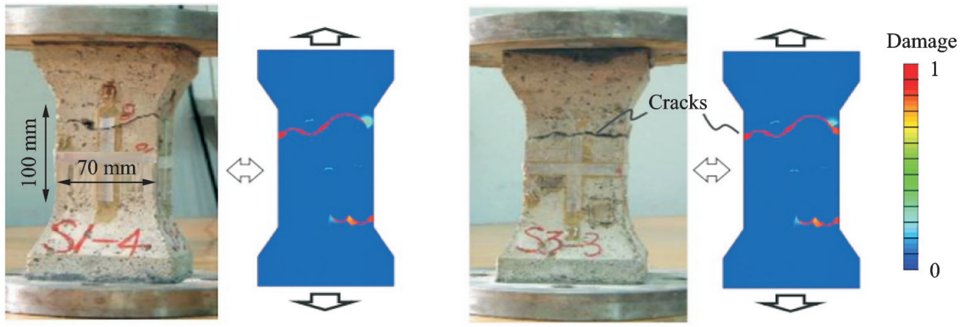

(a) Strain rate: 1×10^{-5} s^{-1} (b) Strain rate: 1×10^{-3} s^{-1}

Fig.4 Comparison of the failure modes of Yan and Lin's[39] test observations and simulation results

crete. This method would be utilized to research the influence of MAS on the tensile and compressive behavior of concrete for further works. Nevertheless, there were errors in the failure modes of Yan and Lin's test observations and simulation results. They might be caused by the discreteness of simulation results.

2 Dynamic Failure Behavior

To explore the influence of MAS on the dynamic failure behavior of concrete material and corresponding dynamic SE, the double-edge notched tensile models and square compressive models having different MAS were established. In this study, the width b of tensile models was 100, 200, 300 and 400 mm. The widths b of compressive models were 100, 150, 300 and 450 mm. Moreover, the applied strain rates were $\dot{\varepsilon}=10^{-5}$, 10^{-4}, 10^{-3}, 10^{-2}, 10^{-1} and 1 s^{-1}. Similar to Bischoff and Perry's reports[40], the applied strain rate of 10^{-5} s^{-1} was assumed the quasi-static condition in this study.

2.1 Failure modes

Fig.5 exhibits the failure modes of concrete specimens having different MAS ($D_{\max}^{\mathrm{agg}}=10$, 20 and 30 mm) under $\dot{\varepsilon}=10^{-2}$ s^{-1}. The damage factor d ($d=1$ for complete damage, and $d=0$ for no damage) was utilized to describe the degree of damage. As seen from Fig.5(a), the internal area having relatively weak mechanical properties (especially the ITZs) firstly reaches damage and then the damage spreads to the mortar matrix under uniaxial tensile loads. Finally, one or two tortuous cracks with a certain width appear near the notch in concrete specimens having different MAS. In addition, MAS significantly affects tensile failure modes of concrete specimens. As the MAS increases, damage cracks near the notch change from straight to tortuous.

Furthermore, it can be seen from Fig. 5(b) that the damage inside concrete specimen is not uniform because of the heterogeneity of concrete material under uniaxial compression. The cracks run diagonally through the specimens and a brittle shear failure in concrete specimens with different MAS could be clearly observed. Similar to the tensile failure modes of concrete, when the concrete is under compressive loads, the damage shows up first in the ITZs and then extended to the mortar matrix of concrete. The damage of all models bypassed aggregates and curved cracks formed eventually. In addition, concrete specimens with large-sized aggregates exhibit discontinuous failure modes. With the MAS decreases, the penetrating crack easily forms in concrete. In general, it can be concluded that the MAS has a hindrance for the development of concrete cracks and affects the failure process of concrete.

Fig.6 shows the final failure modes of concrete specimens (maximum aggregate size $D_{\max}^{\mathrm{agg}}=10$ mm) with different structural sizes under $\dot{\varepsilon}=10^{-3}$ s^{-1}. From Fig.6(a) it can be seen that the crack propagates near the notch of concrete specimens until the whole concrete specimen has been penetrated. In general, concrete specimens with different structural sizes have similar failure patterns under uniaxial tension. Fig. 6(b) exhibits the compressive failure modes of concrete specimens with different structural sizes. As can be observed from Fig. 6 (b), the shear failure modes can be obviously observed. Moreover, the number of cracks increases as the structural size increases.

Fig.7 exhibits the influence of strain rate on the tensile and compressive failure modes of concrete specimens with the structural size of 100 mm × 200 mm and the MAS of 20 mm. Only one crack generates near the notch of concrete specimen under tension when concrete specimen gets damaged under quasi-static load ($\dot{\varepsilon}=10^{-5}$ s^{-1}). With the strain rate increases, the crack becomes more curved and the damage area increases significantly. Similarly, as the strain rate increases, damage inside concrete specimen becomes more and more serious under uniaxial compression. When $\dot{\varepsilon}=10^{-5}$ s^{-1}, only a small amount of areas in ITZs and mortar matrix are crushed. As the strain rate increases, the cracks penetrate through aggregate particles and finally run through the concrete specimens. In general, as the strain rate increases, the internal viscous effect of

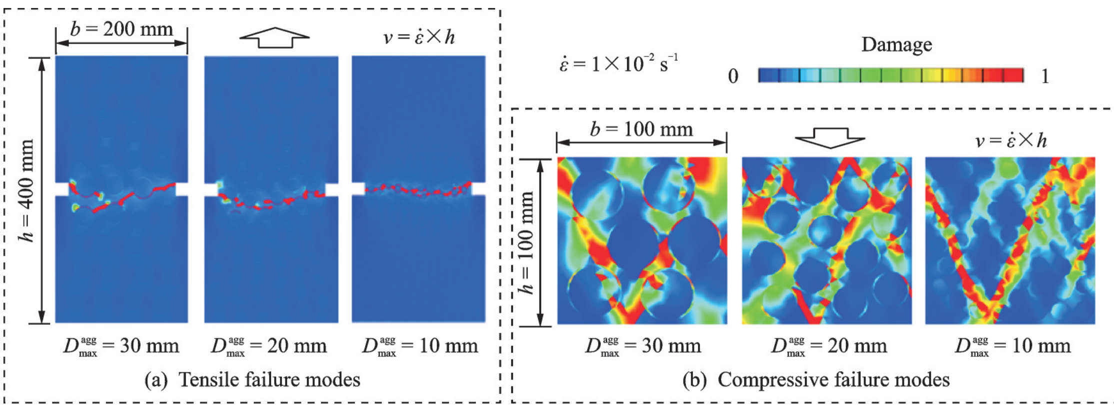

Fig.5 Failure modes of concrete specimens with different aggregate sizes

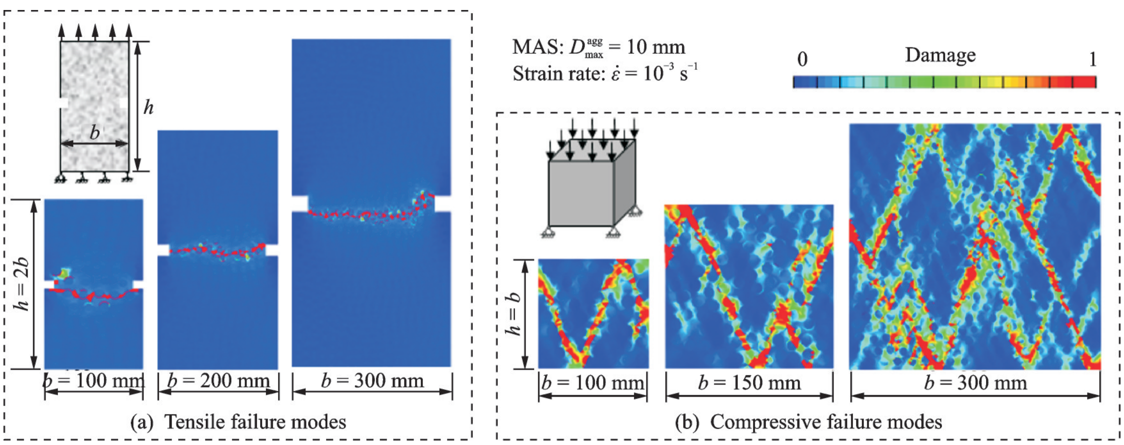

Fig.6 Failure modes of concrete specimens of different specimen sizes

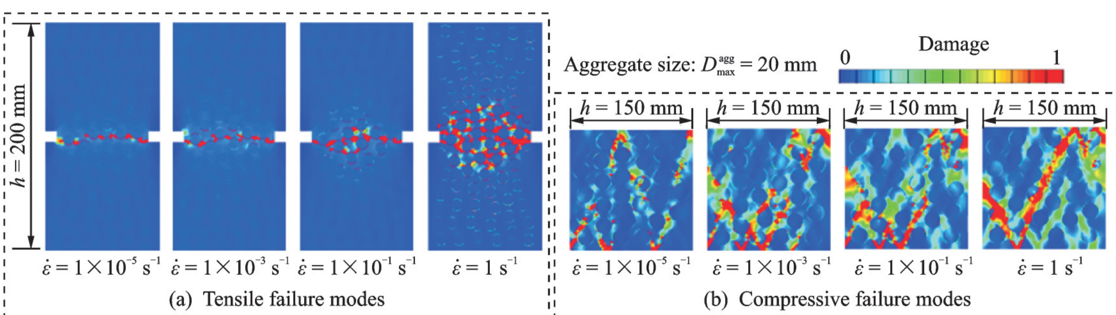

Fig.7 Failure modes of concrete specimens under different strain rates

concrete specimens gradually weakens while the inertia effect gradually becomes the dominant role. As the strain rate increases, there is more serious damage in concrete specimens.

2.2 Stress-strain relations

Fig.8 plots the dynamic stress-strain curves of concrete specimens with structural size of 200 mm × 400 mm, different strain rates and different MAS. Under tensile loads, the peak tensile stress (i.e. tensile strength) and the corresponding peak tensile strain increase with the MAS increases. When $\dot{\varepsilon}=10^{-5}\ \mathrm{s}^{-1}$, the tensile strength of concrete specimens having different MAS has obvious differences and the tensile stress suddenly drops after reaching the peak stress, presenting an obvious brittle failure behavior. As the strain rate increases, the tensile strength of concrete specimens with different MAS has little difference and the ductility of concrete specimens increases due to the increasing damage, showing a significant damage softening effect.

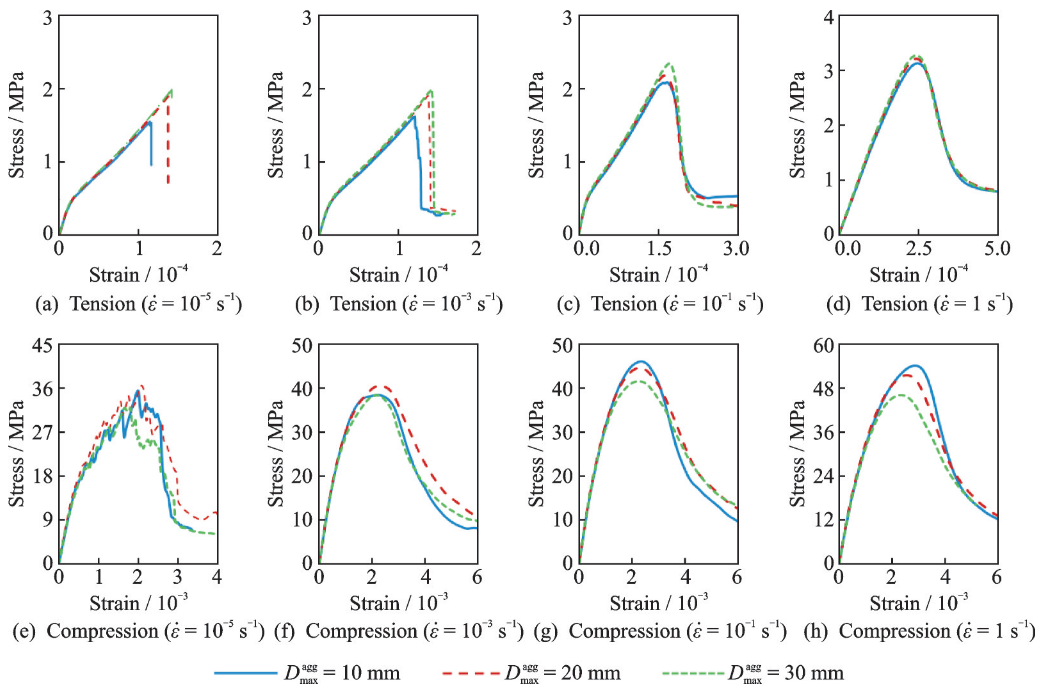

Fig.8 Stress-strain curves of concrete specimens

Under compressive loads, the compressive peak stress (i.e. compressive strength) of concrete specimens having different MAS exhibits different variation laws and the variation laws also change with the increasing strain rate. When $\dot{\varepsilon}\leqslant 10^{-3}\ \mathrm{s}^{-1}$, the compressive strength of concrete specimens having MAS of 20 mm is the maximum one. However, when $10^{-3}\ \mathrm{s}^{-1}<\dot{\varepsilon}\leqslant 1\ \mathrm{s}^{-1}$, As the MAS increases, the compressive strength decreases. In general, the influence of MAS on concrete strength is constantly changing as the applied strain rate varies. Apparently, the influence mechanism of strain rate and MAS on nominal strength is still worth further exploration.

3 Influence of MAS on Size Effect

3.1 Influence of MAS on nominal strength

Fig.9 depicts the variation of nominal strengths of concrete specimens having different MAS and structural sizes under different strain rates. With the MAS increases, the nominal strength increases under uniaxial tensile loads. In addition, the tensile strengths of concrete specimens with different structural sizes vary with the MAS. In general, the increasing trend (i.e. the tensile strength increases with the increasing MAS) is getting slower with the addition of structural size.

However, the MAS performs a different influence on the compressive strength of concrete speci-

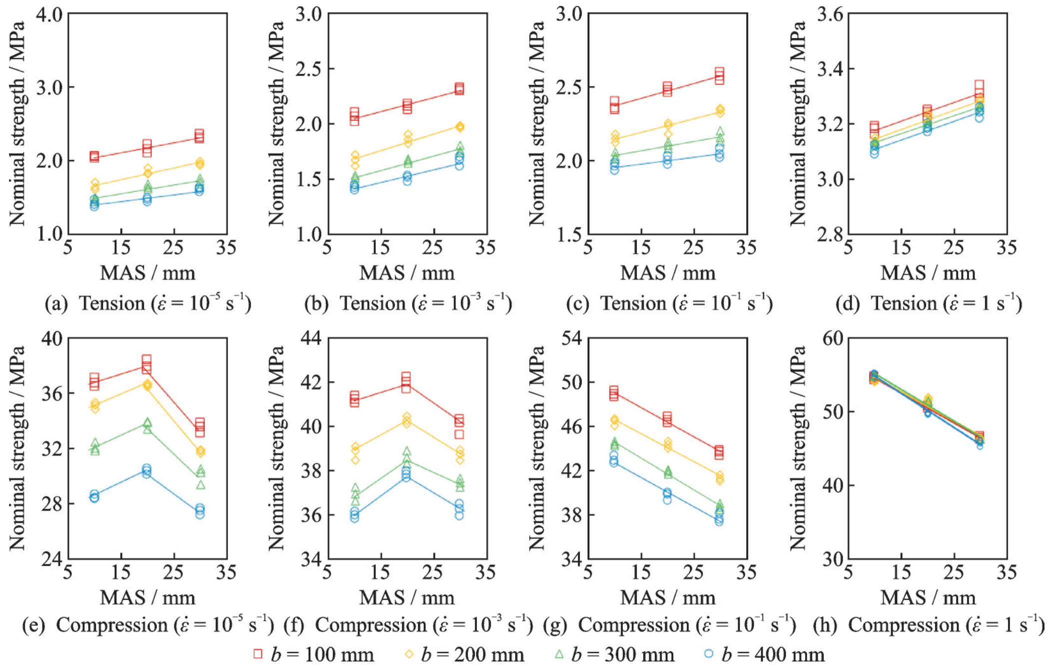

Fig.9 Influence of different MAS on nominal strength of concrete specimens

mens having different structural sizes. When $\dot{\varepsilon} \leqslant 10^{-3}$ s^{-1}, the concrete compressive strength increases first and then decreases suddenly with the increasing MAS. The concrete specimens with the MAS of 20 mm have the maximum compressive strength. However, when 10^{-3} s$^{-1} < \dot{\varepsilon} \leqslant 1$ s^{-1}, the compressive strength of concrete decreases as the MAS increases. This illustrates that the influence of MAS on the compressive strength of concrete changes with the applied strain rate varies.

3.2 Influence of MAS on dynamic size effect

The influence of MAS on concrete SE under different strain rates are obvious in Fig.10. A significant SE on concrete nominal strength can be observed under quasi-static load, i. e. the concrete strength decreases as the structural size increases under uniaxial tensile and compressive loads. However, the decreasing trend becomes slower with the in-

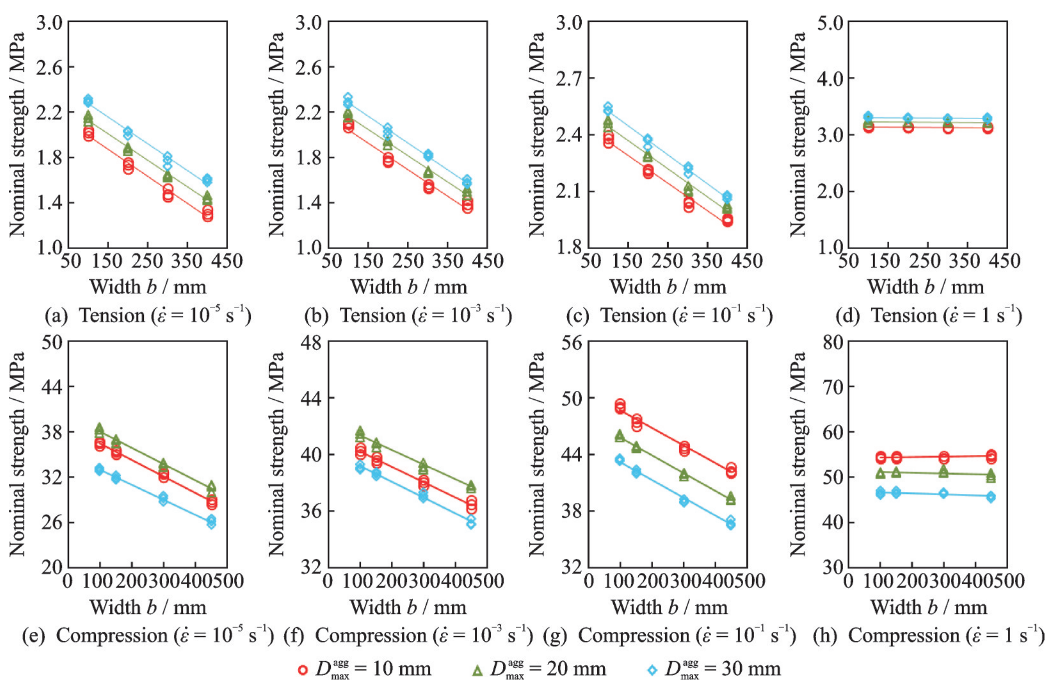

Fig.10 Influence of aggregate sizes on size effect of concrete under different strain rates

creasing strain rate. This indicates that the strain rate has an inhibitory effect on the size effect in concrete. When the applied strain rate reaches 1 s^{-1}, the nominal strength (both tensile strength and compressive strength) of concrete specimen basically remains unchanged with the change in structural size, and the corresponding size effect completely disappears. In addition, the trend line obtained by fitting data is almost parallel with concrete specimens with different MAS. This illustrates that the MAS has an ignorable influence on the dynamic size effect of the concrete under uniaxial tensile and compressive loads.

Combined with the meso-scale numerical method, the dynamic SEL of concrete is discussed briefly at the meso-scale level in this part. Under the uniaxial loads, many meso-cracks generate in the area having weak mechanical properties inside concrete specimen (e.g. the ITZs). With the load increases, cracks continue to expand. However, it is relatively difficult for cracks to penetrate aggregate particles having strong mechanical properties. Therefore, the crack is very likely to bypass the coarse aggregates. In addition, for the double-notched tensile specimens, the tensile nominal strength increases with the MAS increases because the coarse aggregate particles hinder the development of cracks. Conversely, cracks appear randomly inside concrete specimen under uniaxial compression, so that there is an optimum MAS to maximize the compressive strength of concrete.

3.3 Comparison with Bazant's SEL

As mentioned above, many researchers have proposed a series of static SE theories of concrete material[1,4-5]. Here in this part, the classical Bazant's SEL based on the fracture mechanics was utilized[1], and the corresponding theoretical formula can be written as

$$\sigma_{\mathrm{Nu}}=\frac{Bf'}{\sqrt{1+D/D_0}} \tag{1}$$

where σ_{Nu} is the nominal strength; f' the tensile strength (f_t') or compressive strength (f_c') of concrete specimen; D the structural size (herein D is width b of the specimen), and D_0 and B are two empirical constant coefficients, which can be determined by regression analysis based on the simulated results.

For a comparative analysis between the dynamic strength obtained by numerical simulation and the SEL proposed by Bažant, the mathematical transformation of Eq.(1) is given as

$$\left(\frac{f'}{\sigma_{\mathrm{Nu}}}\right)^2=\frac{D}{D_0B^2}+\frac{1}{B^2} \tag{2}$$

Convert Eq.(2) into a linear form as

$$y=Ax+C \tag{3}$$

where $x=D$, $y=(f'/\sigma_{\mathrm{Nu}})^2$, $A=1/D_0B^2$, $C=1/B^2$. Herein, f' is the concrete strength with the width of 100 mm under quasi-static load and the detailed values are shown in Table 2. Table 3 lists the empirical parameters obtained by regression analysis under different strain rates. Consequently, the numerical results compared with the Bazant's SEL, plastic strength criteria (horizontal line) and the linear elastic fracture mechanics (LEFM) are plotted in Fig.11. The most numerical data of concrete specimens generally vary along the curve of Bazant's SEL, illustrating that Bazant's SEL can well describe the influence of structural size on the dynamic strength of concrete. Moreover, the data points gradually approach the line of plastic strength criteria with the increasing strain rate, demonstrating that the size effect of concrete is gradually weakened.

Table 2 Strength of concrete specimens with the width of 100 mm under quasi-static load

MAS /mm	Tensile strength /MPa	Compressive strength / MPa
10	2.05	36.72
20	2.15	37.90
30	2.31	32.48

3.4 Verification of Jin et al.'s size effect law

As mentioned previously, Jin et al.[19-20] have set up a meso-scale numerical method to explore the dynamic size effect of concrete under dynamic compressive and tensile loads, and a unified SEL which can describe the influence of structural size on concrete strength under static and dynamic loads has

Table 3 Value of parameters B and D_0 under different strain rates

$\dot{\varepsilon}$ /s^{-1}	D_{agg} / mm	Tensile parameter					Compression parameter				
		A	C	Bf_t' / MPa	B	D_0/mm	A	C	Bf_c' / MPa	B	D_0/mm
10^{-5}	10	9.80×10^{-4}	1.61×10^{-1}	2.49	1.215	161	1.43×10^{-6}	5.83×10^{-4}	41.42	1.128	407
	20	8.38×10^{-4}	1.21×10^{-1}	2.89	1.344	150	1.13×10^{-6}	5.80×10^{-4}	41.53	1.096	514
	30	6.82×10^{-4}	1.22×10^{-1}	2.89	1.251	171	1.09×10^{-6}	8.32×10^{-4}	34.67	1.067	762
10^{-3}	10	1.03×10^{-3}	1.49×10^{-1}	2.59	1.257	149	4.49×10^{-7}	5.83×10^{-4}	41.42	1.128	1 299
	20	8.17×10^{-4}	1.24×10^{-1}	2.85	1.326	154	3.65×10^{-7}	5.82×10^{-4}	42.55	1.123	1 514
	30	6.52×10^{-4}	1.18×10^{-1}	2.92	1.264	168	3.72×10^{-7}	6.08×10^{-4}	40.55	1.248	1 634
10^{-1}	10	2.59×10^{-4}	1.61×10^{-1}	2.49	1.042	537	3.03×10^{-7}	4.05×10^{-4}	49.67	1.353	1 336
	20	2.65×10^{-4}	1.46×10^{-1}	2.62	1.056	487	5.20×10^{-7}	4.16×10^{-4}	49.03	1.294	801
	30	2.70×10^{-4}	1.30×10^{-1}	2.78	1.094	432	4.56×10^{-7}	5.08×10^{-4}	44.37	1.366	1 114
1	10	7.89×10^{-6}	9.97×10^{-2}	3.17	1.003	12463	1.98×10^{-9}	3.40×10^{-4}	54.21	1.476	171 489
	20	8.74×10^{-6}	9.44×10^{-2}	3.25	1.000	10489	3.61×10^{-8}	3.77×10^{-4}	51.52	1.359	10 436
	30	5.16×10^{-6}	9.21×10^{-2}	3.30	1.003	18420	2.85×10^{-8}	4.65×10^{-4}	46.38	1.428	16 341

f_t' is the tensile strength of concrete having width of 100 mm under the strain rate of 1×10^{-5} s^{-1}: when $D_{max}^{agg}=10$, 20 and 30 mm, $f_t'=2.05$, 2.15 and 2.31 MPa, respectively; f_c' is the compressive strength of concrete with width of 100 mm under the strain rate of 1×10^{-5} s^{-1}: when $D_{max}^{agg}=10$, 20 and 30 mm, $f_c'=36.72$, 37.90 and 32.48 MPa, respectively.

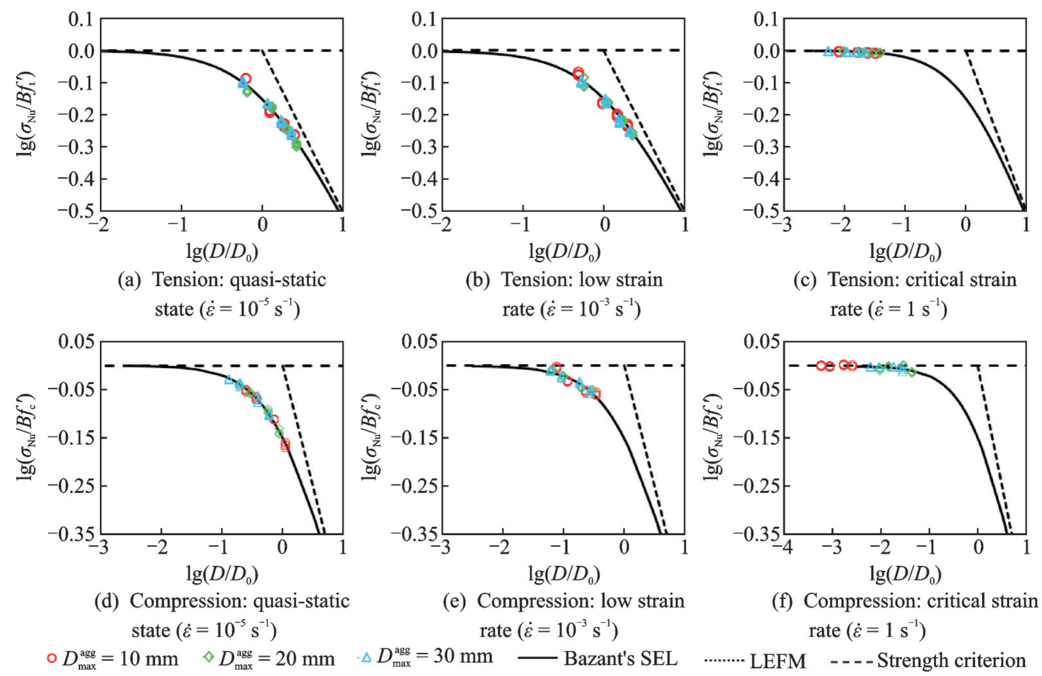

Fig.11 Comparison of numerical results and size effect theory

been built. The unified SEL proposed by Jin et al.[19-20] can be expressed as

$$\sigma_{Nu}=\frac{Bf'}{\sqrt{1+D/D_0}}\cdot\varphi\cdot\beta \tag{4}$$

where f' = the simulated nominal strength of the concrete having a certain structural size (standard specimen); φ = the strength enhancement coefficient (φ = TDIF for tensile models and φ = CDIF for compressive models) obtained from the simulation results. Fig. 12 exhibits the fitting formulas of TDIF and CDIF. β is the influence coefficient of strain rate on size effect on concrete strength, it can be specifically written as

$$\beta=1 \quad \dot{\varepsilon}\leqslant10^{-5}\ \mathrm{s}^{-1} \tag{5a}$$

$$\beta=\left(\frac{\sqrt{1+D/D_0}}{25B}-\frac{1}{25}\right)\cdot\left(\lg\dot{\varepsilon}+5\right)^2+1$$

$$10^{-5}\ \mathrm{s}^{-1}<\dot{\varepsilon}\leqslant1\ \mathrm{s}^{-1} \tag{5b}$$

Fig.13 plots the comparison of the simulated results and the predicted results based on the theoretical formula proposed by Jin et al.[19-20]. One can note from Fig.13 that most simulated data points basically agree well with the theoretical results, which verifies the rationality of simulated results and the applicability of meso-scale numerical method.

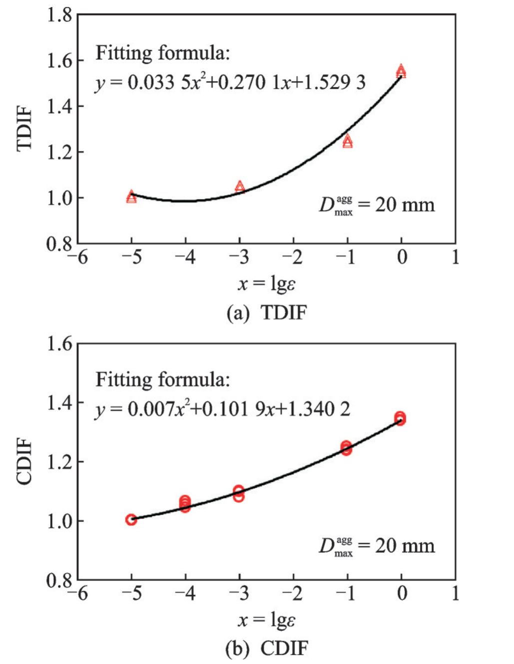

Fig.12 Fitting curve for the DIF of dynamic strengths of standard specimens

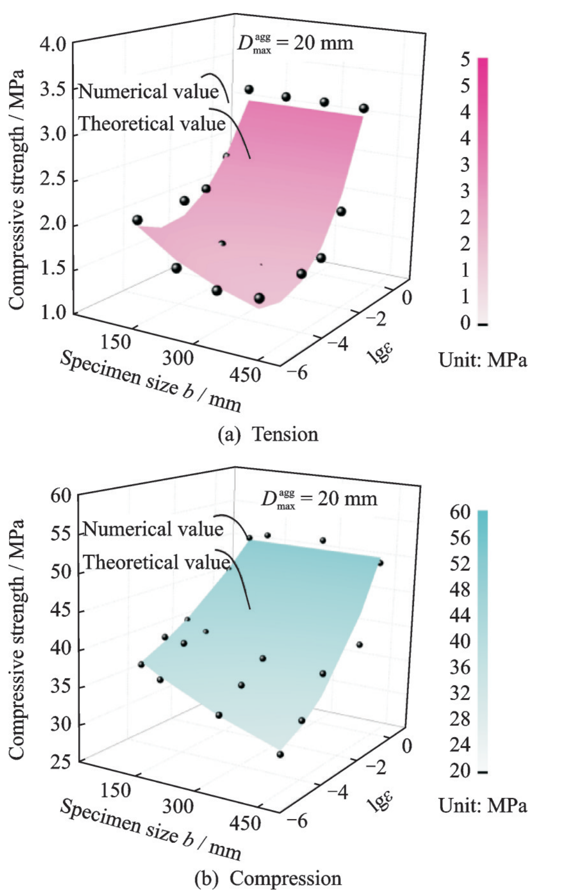

Fig.13 Comparison of the numerical and theoretical results

4 Conclusions

In the present study, a series of meso-scale numerical simulations were performed to investigate the dynamic mechanical behavior and corresponding dynamic size effect of concrete specimens having different MAS under low strain rates. The numerical results reveal that the MAS and strain rate have a significant influence on the failure behavior of concrete material under uniaxial tensile and compressive loads. The influence mechanism of MAS on the nominal strength and corresponding dynamic size effect of concrete material has been analyzed. The conclusion can be summarized as follows:

(1) MAS has an obvious influence on the failure modes of concrete under compressive and tensile loads. The smaller the MAS, the more serious the internal damage of concrete material.

(2) Under quasi-static load, the tensile strength of concrete increases as the MAS increases while the nominal compressive strength of concrete increases first and then decreases as the MAS increases.

(3) The size effect of concrete is weakened as the strain rate increases. When the applied strain rate reaches 1 s^{-1}, the size effect completely disappears.

(4) MAS has an ignorable influence on the dynamic SE of concrete under compressive and tensile loads.

It should be noted that only the numerical simulations for exploring the influence of MAS on mechanical behavior of concrete are far from enough. More tests should be performed to verify the accuracy of the simulated results in future works. Moreover, more factors (e.g. aggregate content, aggregate shape, aggregate distribution, etc.) should also be further considered.

References

[1] BAZANT Z P, PLANAS J. Fracture and size effect in concrete and other quasi-brittle materials[M]. Boca

Raton, USA: CRC Press, 1998: 7-15.

[2] DU X, JIN L. Meso-element equivalent model for macro-scopic mechanical properties analysis of concrete materials[J]. Chinese Journal of Computational Mechanics, 2012, 29(5): 654-661.

[3] DU X, JIN L, MA G. A meso-scale analysis method for the simulation of nonlinear damage and failure behavior of reinforced concrete members[J]. International Journal of Damage Mechanics, 2013, 22(6): 878-904.

[4] WEIBULL W. The phenomenon of rupture in solids[J]. IVA Handlingar, 1939, 153: 1-55.

[5] CARPINTERI A, FERRO G. Size effects on tensile fracture properties: A unified explanation based on disorder and fractality of concrete microstructure[J]. Materials and Structures, 1994, 27(10): 563-571.

[6] NEVILLE A M. Properties of concrete[M]. London: Longman, 1995.

[7] SIM J, YANG K, JEON J. Influence of aggregate size on the compressive size effect according to different concrete types [J]. Construction and Building Materials, 2013, 44:716-725.

[8] TASDEMIR C, TASDEMIR M A, LYDON F D, et al. Effects of silica fume and aggregate size on the brittleness of concrete[J]. Cement and Concrete Research, 1996, 26(1): 63-68.

[9] RAO G A, PRASAD B K R. Fracture energy and softening behavior of high-strength concrete[J]. Cement and Concrete Research, 2002, 32(2): 247-252.

[10] LI Q, DENG Z, FU H. Effect of aggregate type on mechanical behavior of dam concrete[J]. Materials Journal, 2004, 101(6): 483-492.

[11] CHEN B, LIU J. Effect of aggregate on the fracture behavior of high strength concrete[J]. Construction and Building Materials, 2004, 18(8): 585-590.

[12] ZHANG J, LIU Q, WANG L. Effect of coarse aggregate size on relationship between stress and crack opening in normal and high strength concretes[J]. Journal of Materials Science and Technology, 2005, 21(5): 691-700.

[13] AL-ORAIMI S K, TAHA R, HASSAN H F. The effect of the mineralogy of coarse aggregate on the mechanical properties of high-strength concrete[J]. Construction and Building Materials, 2006, 20(7): 499-503.

[14] FU H C, ERKI M A, SECKIN M. Review of effects of loading rate on concrete in compression[J]. Journal of Structural Engineering, 1991, 117(12): 3645-3659.

[15] PARK S W, XIA Q, ZHOU M. Dynamic behavior of concrete at high strain rates and pressures: II. Numerical simulation[J]. International Journal of Impact Engineering, 2001, 25(9): 887-910.

[16] KRAUTHAMMER T, ELFAHAL M M, LIM J, et al. Size effect for high-strength concrete cylinders subjected to axial impact[J]. International Journal of Impact Engineering, 2003, 28(9): 1001-1016.

[17] WANG X, ZHANG S, WANG C, et al. Experimental investigation of the size effect of layered roller compacted concrete (RCC) under high-strain-rate loading[J]. Construction and Building Materials, 2018, 165: 45-57.

[18] ELFAHAL M M, KRAUTHAMMER T. Dynamic size effect in normal-and high-strength concrete cylinders[J]. ACI Materials Journal, 2005, 102(2): 77.

[19] JIN L, YU W, DU X, et al. Meso-scale modelling of the size effect on dynamic compressive failure of concrete under different strain rates[J]. International Journal of Impact Engineering, 2019, 125: 1-12.

[20] JIN L, YU W, DU X, et al. Mesoscopic numerical simulation of dynamic size effect on the splitting-tensile strength of concrete[J]. Engineering Fracture Mechanics, 2019, 209: 317-332.

[21] ZHOU X Q, HAO H. Modelling of compressive behaviour of concrete-like materials at high strain rate[J]. International Journal of Solids and Structures, 2008, 45(17): 4648-4661.

[22] DU X, JIN L. Meso-scale numerical investigation on cracking of cover concrete induced by corrosion of reinforcing steel[J]. Engineering Failure Analysis, 2014, 39: 21-33.

[23] DU X, JIN L, MA G. Meso-element equivalent method for the simulation of macro mechanical properties of concrete[J]. International Journal of Damage Mechanics, 2013, 22(5): 617-642.

[24] ROSSIGNOLO J A, AGNESINI M V C. Durability of polymer-modified lightweight aggregate concrete[J]. Cement and Concrete Composites, 2004, 26(4): 375-380.

[25] DU X, JIN L, MA G. Numerical simulation of dynamic tensile-failure of concrete at meso-scale[J]. International Journal of Impact Engineering, 2014, 66: 5-17.

[26] SADOUKI H, WITTMANN F H. On the analysis of the failure process in composite materials by numerical simulation[J]. Materials Science and Engineering: A, 1988, 104: 9-20.

[27] CUSATIS G, MENCARELLI A, PELESSONE D, et al. Lattice discrete particle model (LDPM) for failure behavior of concrete. II: Calibration and validation[J]. Cement and Concrete Composites, 2011, 33(9): 891-905.

[28] GRASSL P, GRÉGOIRE D, SOLANO L R, et al.

Meso-scale modelling of the size effect on the fracture process zone of concrete[J]. International Journal of Solids and Structures, 2012, 49(13): 1818-1827.

[29] JIN L, XU C, HAN Y, et al. Effect of end friction on the dynamic compressive mechanical behavior of concrete under medium and low strain rates[J]. Shock and Vibration, 2016, 2016: 6309073.

[30] GROTE D L, PARK S W, ZHOU M. Dynamic behavior of concrete at high strain rates and pressures: I. experimental characterization[J]. International Journal of Impact Engineering, 2001, 25(9): 869-886.

[31] LEE J, FENVES G L. Plastic-damage model for cyclic loading of concrete structures[J]. Journal of Engineering Mechanics, 1998, 124(8): 892-900.

[32] DILGER W H, KOCH R, KOWALCZYK R. Ductility of plain and confined concrete under different strain rates[J]. Journal Proceedings, 1984, 81(1): 73-81.

[33] BISCHOFF P H, PERRY S H. Compressive behaviour of concrete at high strain rates[J]. Materials and Structures, 1991, 24(6): 425-450.

[34] HAO Y, HAO H, LI Z. Influence of end friction confinement on impact tests of concrete material at high strain rate[J]. International Journal of Impact Engineering, 2013, 60: 82-106.

[35] CEB-FIP M C. Model code for concrete structures[M]. USA: Bulletin D'Information, 1990.

[36] MALVAR L J, ROSS C A. Review of strain rate effects for concrete in tension[J]. ACI Materials Journal, 1998, 95(6): 735-739.

[37] BAŽANT Z P, CANER F C, ADLEY M D, et al. Fracturing rate effect and creep in microplane model for dynamics[J]. Journal of Engineering Mechanics, 2000, 126(9): 962-970.

[38] CHEN X, WU S, ZHOU J. Experimental and modeling study of dynamic mechanical properties of cement paste, mortar and concrete [J]. Construction and Building Materials, 2013, 47: 419-430.

[39] YAN D, LIN G. Dynamic properties of concrete in direct tension[J]. Cement and Concrete Research, 2006, 36(7): 1371-1378.

[40] BISCHOFF P H, PERRY S H. Compressive behavior of concrete at high strain rates[J]. Materials and Structures, 1991, 24(6): 425-450.

Acknowledgements This work was supported by the National Key Basic Research and Development Program of China (No. 2018YFC1504302) and the National Natural Science Foundation of China (Nos. 51822801, 51421005).

Authors Prof. **JIN Liu** received his Ph.D. degrees from Beijing University of Technology in 2014. From 2016 to present, he is a doctoral supervisor in Beijing University of Technology. His research has focused on the concrete engineering structures.

Prof. **DU Xiuli** received his Ph.D. degree from Institute of Engineering Mechanics, Chinese Academy of Sciences in 1990. From 2014 to now, he is the Vice President of Beijing University of Technology. His research has focused on the earthquake resistance and explosion resistance of building structures.

Author contributions Prof. **JIN Liu** reviewed and revised the paper; Mr. **YANG Wangxian** conducted the simulation and wrote the paper; Mr. **YU Wenxuan** analyzed the data; and Prof. **DU Xiuli** reviewed the paper and provided advices. All authors approved the submission.

Competing interests The authors declare no competing interests.

(Production Editor: ZHANG Bei)

低应变率下最大骨料粒径对混凝土动态尺寸效应影响:细观模拟

金 浏,杨旺贤,余文轩,杜修力

(北京工业大学城市与工程安全减灾教育部重点实验室,北京 100124,中国)

摘要:本文主要探讨了低应变率下最大骨料粒径对混凝土材料破坏行为及尺寸效应的影响。首先,考虑混凝土材料内部的非均匀性和应变率效应,采用细观数值方法模拟了混凝土材料的破坏过程。基于细观数值模拟方法,研究了不同尺寸混凝土试件的破坏行为。其次,从细观层面上研究了最大骨料粒径对混凝土破坏模式、名义强度及其尺寸效应的影响规律。结果表明,在单轴压缩和拉伸载荷作用下最大骨料粒径对混凝土破坏模式有显著影响。在准静态荷载作用下,混凝土抗拉强度随着最大骨料粒径的增大而增大,抗压强度随着最大骨料粒径的增大则是先增大后减小。此外,随着应变率的增大,混凝土材料强度尺寸效应被逐渐减弱。当应变率达到 1 s^{-1}时,混凝土强度尺寸效应消失。最大骨料粒径对混凝土单轴压缩和拉伸强度动态尺寸效应的影响可忽略。

关键字:混凝土;最大骨料粒径;尺寸效应;动态压缩;动态拉伸;应变率